REPORT DOCUMENTATION PAGE

Form Approved OMB NO. 0704-0188

1. REPORT DATE (DD-MM-YYYY)	2. REPORT TYPE	3. DATES COVERED (From - To)
07-11-2014	Related Material	-

4. TITLE AND SUBTITLE
Temperature Dependent Photoluminescence of CuInS2 with ZnS Capping

5a. CONTRACT NUMBER
W911NF-11-1-0177

5b. GRANT NUMBER

5c. PROGRAM ELEMENT NUMBER
206022

6. AUTHORS
Quinn Allen Hailes Jr.

5d. PROJECT NUMBER

5e. TASK NUMBER

5f. WORK UNIT NUMBER

7. PERFORMING ORGANIZATION NAMES AND ADDRESSES
Hampton University
100 E. Queen Street

Hampton, VA 23668 -0108

8. PERFORMING ORGANIZATION REPORT NUMBER

9. SPONSORING/MONITORING AGENCY NAME(S) AND ADDRESS (ES)
U.S. Army Research Office
P.O. Box 12211
Research Triangle Park, NC 27709-2211

10. SPONSOR/MONITOR'S ACRONYM(S)
ARO

11. SPONSOR/MONITOR'S REPORT NUMBER(S)
58943-EL-REP.12

12. DISTRIBUTION AVAILIBILITY STATEMENT
Approved for public release; distribution is unlimited.

13. SUPPLEMENTARY NOTES
The views, opinions and/or findings contained in this report are those of the author(s) and should not contrued as an official Department of the Army position, policy or decision, unless so designated by other documentation.

14. ABSTRACT
The commercial interest in Cd-free quantum dots for photonic and biomedical applications, has significantly increased in the last ten years. Due to high quantum yield, good spectral distribution, and weak photobleaching, semiconductor nanocrystals (SNCs) of Copper Indium Disulfide (CIS) have been considered for such applications. For CIS SNCs, the optical properties are characteristic of quantum-confined excitons within the nanocrystal boundary, while a notable blue shift from bulk materials is observed. CIS

15. SUBJECT TERMS
Semiconductor Nanocrystals, Optical Spectroscopy

16. SECURITY CLASSIFICATION OF:			17. LIMITATION OF ABSTRACT	15. NUMBER OF PAGES	19a. NAME OF RESPONSIBLE PERSON
a. REPORT	b. ABSTRACT	c. THIS PAGE			Jaetae Seo
UU	UU	UU	UU		19b. TELEPHONE NUMBER 757-727-5149

Report Title

Temperature Dependent Photoluminescence of CuInS2 with ZnS Capping

ABSTRACT

The commercial interest in Cd-free quantum dots for photonic and biomedical applications, has significantly increased in the last ten years. Due to high quantum yield, good spectral distribution, and weak photobleaching, semiconductor nanocrystals (SNCs) of Copper Indium Disulfide (CIS) have been considered for such applications. For CIS SNCs, the optical properties are characteristic of quantum-confined excitons within the nanocrystal boundary, while a notable blue shift from bulk materials is observed. CIS SNCs are highly sensitive to compositions, morphologies, and lattice strains allowing them to display unique optical and electronic properties. Temperature- dependent photoluminescence (PL) studies of CIS and CIS capped with Zinc Sulfide (ZnS) SNCs were carried out in temperatures ranging from 6K – 300K. In this work, PL quenching is observed for various optical transitions that occur in the SNCs which correspond to specific energy transitions within the nanocrystals. Temperature-dependent spectroscopy revealed the interface- defect and surface-defect transitions were thermally active at low temperatures; however for CIS/ZnS the intrinsic-defect states were relatively stable because the strong Coulomb interaction between charge carriers.

Temperature Dependent Photoluminescence of $CuInS_2$ with ZnS Capping

Senior Capstone Thesis

By

Quinn Allen Hailes Jr.

PHY 500

May 11, 2014

This thesis, submitted by Quinn A. Hailes Jr. in partial fulfillment of the requirements for the degree of Bachelor of Science in Physics at Hampton University, Virginia is hereby approved by the committee under whom the work has been completed.

_____

Mahmoud Abdel-Fattah, Ph.D.
Primary Research Advisor

_____

Donald A. Whitney, Ph.D.
Interim Chairman, Department of Physics

ABSTRACT

Temperature Dependent Photoluminescence of $CuInS_2$ with ZnS Capping

Quinn A. Hailes Jr., Hampton University

April 17, 2014

The commercial interest in Cd-free quantum dots for photonic and biomedical applications, has significantly increased in the last ten years. Due to high quantum yield, good spectral distribution, and weak photobleaching, semiconductor nanocrystals (SNCs) of Copper Indium Disulfide (CIS) have been considered for such applications. For CIS SNCs, the optical properties are characteristic of quantum-confined excitons within the nanocrystal boundary, while a notable blue shift from bulk materials is observed. CIS SNCs are highly sensitive to compositions, morphologies, and lattice strains allowing them to display unique optical and electronic properties. Temperature- dependent photoluminescence (PL) studies of CIS and CIS capped with Zinc Sulfide (ZnS) SNCs were carried out in temperatures ranging from 6K – 300K. In this work, PL quenching is observed for various optical transitions that occur in the SNCs which correspond to specific energy transitions within the nanocrystals. Temperature-dependent spectroscopy revealed the interface- defect and surface-defect transitions were thermally active at low temperatures; however for CIS/ZnS the intrinsic-defect states were relatively stable because the strong Coulomb interaction between charge carriers.

Table of Contents

Page

List of Figures

Page

INTRODUCTION

The next big thing in condensed matter and optical physics research is the nano-sized particle called the quantum dot. Quantum dots are tiny particles, sometimes called nanoparticles, of a semiconductor material. The sizes of these quantum dots usually range from 2 to 10 nanometers in diameter. Louis E. Brus discovered quantum dots in the year of 1980. Due to their small size, quantum dots display unique optical and electrical properties.

Due to the small size of quantum dots, the electrons inside are confined in a small space, which is referred to as a quantum well. When the radius of the semiconductor nanocrystal is smaller than the exciton Bohr radius there is quantization of the energy levels according to Pauli's exclusion principle. The exciton Bohr radius is the average distance between the electron in the conduction band and the hole it leaves behind in the valence band after excitation.

The most obvious characteristic is the emission of photons under excitation, which can be visible to the human eye. Moreover, the wavelength of photo-emission depends not on the material from which the quantum dot is made, but on the size of the quantum dots. Laboratories, who manufacture quantum dots, have the ability to precisely control their size through chemical reaction. Since manufactures have the power to control the size this key factor also determines the wavelength of the emission. This will also conclude the color of light that is observed.

Usually as the size of the quantum dot decreases, the difference in energy between the largest valence band and the lowest conduction band increases. More energy will be required to excite the dot; therefore more energy is released when the dot returns to the

ground state. This results in a color shift from either red or blue in the emitted light depending on the size of the quantum dot. Ultimately quantum dots can be tuned in fabrication to emit any color of light desired. The smaller the quantum dot, the closer it is to the blue end of the light spectrum, and the larger the dot, the closer to the red end of the light spectrum. Quantum dots can even be tuned beyond visible light, into the infrared or into the ultra-violet spectrum. When these nanoparticles are created their outcome is either in powder form or a liquid solution.

Quantum dots can be classified into different types based on their composition and structure. Core-Shell Quantum dots can be made of single component materials with uniform compositions such as chalcogenides of metals like cadmium or zinc like cadmium selenide. The optical properties of core-type nanocrystals can be fine-tuned by changing the quantum dot size. Core-Shell Quantum Dots have a small region of one material embedded in another material that has a larger band gap. The ZnS/CIS used in this experiment is an example of a core-shell quantum dot. The luminescent properties of quantum dots come from the recombination of electron-hole pairs through radiative decay. However, the exciton decay can also occur through nonradiative methods, reducing the fluorescence quantum yield. A way to improve the efficiency and brightness of quantum dots is to grow shells of higher band gap material around them. Lastly, combining together two semiconductors with different band gap energies forms alloyed quantum dots. The synthesis of an alloyed quantum dots is different from the previous two mentioned. When alloyed quantum dots are manufactured they go through an extra annealing process that produces the alloy. Alloyed quantum dots have unique and additional composition properties aside from the properties that come about due to

quantum confinement effects. The unique size and composition tunable properties of these very small quantum dots make them useful in a range of applications and new technology.

In recent years scientists have began intensive research with quantum dots for use in lighting and displays. Currently white-light emitting diodes (LEDs) consist of a blue emitting LED coated with a phosphor that is excited by the LED and emits a yellow or orange light. The mixture of blue and yellow produces a cold white light lacking red photons, therefore many objects looks unnatural under the lighting. There are phosphors that can produce color closer to that of an incandescent light, but they come with a drop in energy efficiency.

Schrodinger Equation: Particle In A 3-Dimensional Box

Quantum dots can be explained as a particle in a three-dimensional box. A box with edge length L is located in the region $0< x, y, z < L$. Classically, a particle would move around inside a box, colliding with the walls. After a collision, the component of particles momentum normal to the wall is reversed (flipped in the opposite direction), while the other two components of momentum are unaffected. The collisions occurring in the box preserve the magnitude of each momentum component, plus the total particle energy. These four quantities $|p_x|$, $|p_y|$, $|p_z|$, and Energy (E) are constants in classical physics and will be used to find quantum states.

A wave function Ψ in quantum mechanics is used to describe the quantum state of a system of one or more particles, and contains all the information about the system. The wave function Ψ in three dimensions is a function of $\mathbf{r}$ and t. The magnitude of Ψ

determines the probability density $P(\mathbf{r}, t) = |\Psi(\mathbf{r}, t)|^2$, which is the probability per unit volume. Multiplying by the volume components dV gives the probability of find the particle within the volume element dV at the point **r** at time *t*.

Quantum Dots can be described like particles that are confined in a box, the wave function Ψ is zero at the walls and outside the box. The wave function inside the box is found from Schrödinger's equation,

$$\frac{-\hbar^2}{2m}\nabla^2\Psi + U(r)\Psi = i\hbar\frac{\partial\Psi}{\partial t} \qquad (1)$$

Since quantum dots are three-dimensional particles the Laplacian operator is used,

$$\nabla^2 = \frac{\partial}{\partial x^2} + \frac{\partial}{\partial y^2} + \frac{\partial}{\partial z^2} \qquad (2)$$

V(**r**) is the potential energy as a function of all the space coordinates: V(**r**) = V(x, y, z). The Laplacian multiplied with the constants is defined as the kinetic energy operator. The left side of equation 1 is defined as the Hamiltonian operator [**H**] applied to Ψ and the right side of the equation is the energy operator [**E**] applied to Ψ.

Stationary states are those for which all probabilities are constant in time, and are given by solutions to Schrödinger's equation in the separable form,

$$\Psi(\mathbf{r}, t) = \phi(\mathbf{r})e^{-i\omega t} \qquad (3)$$

Where the exponential is the time dependent component of the Schrödinger equation and ϕ(**r**) is known as the time-independent Schrödinger equation for a particle whose energy is $E = \hbar\omega$:

$$-\frac{\hbar^2}{2m}\nabla^2\phi(\mathbf{r}) + V(\mathbf{r})\phi(\mathbf{r}) = E\phi(\mathbf{r}) \qquad (4)$$

Since the particle is free inside the box, the potential energy V(**r**) = 0 for 0 < x, y, z < L. To solve the wave function the mathematical technique of separation of variables is used:

$$\phi(\mathbf{r}) = \phi(x, y, z) = \phi_1(x)\phi_2(y)\phi_3(z) \qquad (5)$$

Substituting equation 5 into equation 4 and dividing every term by the ϕ(x, y, z) gives {V(**r**) = 0}

$$-\frac{\hbar^2}{2m}\frac{1}{\phi_1}\frac{d^2\phi_1}{dx^2} - \frac{\hbar^2}{2m}\frac{1}{\phi_2}\frac{d^2\phi_2}{dy^2} - \frac{\hbar^2}{2m}\frac{1}{\phi_3}\frac{d^2\phi_3}{dz^2} = E \qquad (6)$$

In this form the independent variables (x, y, z) are isolated: the first term on the left only depends on x, the second only depends on y, and the third only depends on z. To satisfy the equations everywhere inside the cube, each of the these terms must be equal to a constant:

$$\begin{aligned} -\frac{\hbar^2}{2m}\frac{1}{\phi_1}\frac{d^2\phi_1}{dx^2} &= E_1 \\ -\frac{\hbar^2}{2m}\frac{1}{\phi_2}\frac{d^2\phi_2}{dy^2} &= E_2 \\ -\frac{\hbar^2}{2m}\frac{1}{\phi_3}\frac{d^2\phi_3}{dz^2} &= E_3 \end{aligned} \qquad (7)$$

The stationary states for a particle confined in a box are gathered from these three separate equations. The energies E_1, E_2, and E_3 represent the energy of motion along the three Cartesian axes x, y, and z respectively. Consistent with this identification because of the superposition principle, the Schrödinger equation entails that $E_1 + E_2 + E_3 = E$

The first of equations 7 is the same as a one-dimensional particle for an infinite square well. The general solution for that equation is $\sin xk_1 + \cos xk_1$ where $k_1 = \sqrt{((2mE_1)/\hbar^2)}$ is the wavenumber of oscillations. However only "sine" meets the boundary condition for the wave function, that must disappear at the wall x = 0. This

also makes the wave function disappear at the other end of the wall x = L implying k_1 L= $n_1\pi$ where, n_1 can be any positive integer. In short, one must fit an integral number of half-wavelengths into the box along the direction marked by x for this example. The magnitude of a particle momentum along the x direction must have discrete values

$$|p_x| = \hbar k_1 = n_1 \frac{\pi\hbar}{L} \qquad n_1 = 1, 2, \ldots \qquad (9)$$

This will be identical for the remaining to equations in the y and z direction. The magnitudes of the particles momentum in all three directions are similarly quantized:

$$\begin{aligned} |p_x| &= \hbar k_1 = n_1 \frac{\pi\hbar}{L} \qquad n_1 = 1, 2, \ldots \\ |p_y| &= \hbar k_2 = n_2 \frac{\pi\hbar}{L} \qquad n_2 = 1, 2, \ldots \qquad (10) \\ |p_z| &= \hbar k_3 = n_3 \frac{\pi\hbar}{L} \qquad n_3 = 1, 2, \ldots \end{aligned}$$

$n_i = 0$ is not allowed because that value leads to a Φ that is also zero and a wave function $\Phi(\mathbf{r})$ that doesn't exist. The particle kinetic energy is limited to the following discrete values:

$$\begin{aligned} E &= \frac{1}{2m}\left(|p_x|^2 + |p_y|^2 + |p_z|^2\right) \\ &= \frac{\pi^2\hbar^2}{2mL^2}\left(n_1^2 + n_2^2 + n_3^2\right) \qquad (11) \end{aligned}$$

Confining a particle in a three-dimensional box serves to quantize its momentum and energy shown by equation 10 and equation 11. Three quantum numbers are needed to specify the quantum condition, corresponding to the three independent degrees of freedom for a particle in space. When all equations above are gathered the wave function Ψ describes the behavior of a particle confined in a three-dimensional box at a given time:

$$\Psi(x,y,z,t) = A\sin(k_1 x)\sin(k_2 y)\sin(k_3 z)e^{-iwt} \qquad for\ 0 < x,y,z < L$$
$$= 0 \qquad otherwise$$

The constant A is chosen to satisfy the normalization requirement. Any wave function must be continuous, normalize-able, and differentiable.

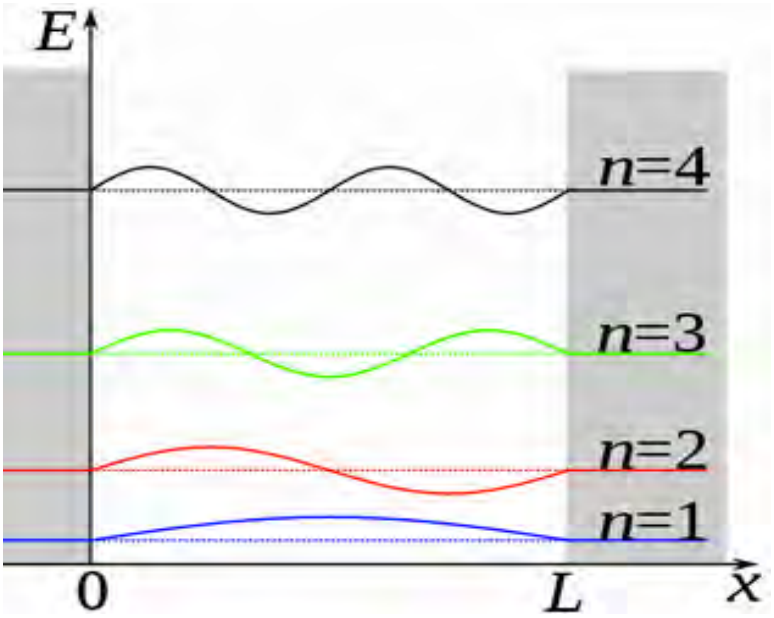

Figure 1. Energy Levels of particle in box

When looking at the various energy levels of excited quantum dots, they can display different energy transitions depending on the defect that is related to the surface imperfections. In semiconductor nanocrystals there are three transitional defects that can occur after the absorbance of energy, which is surface, shallow, and deep. In figure 2 the energy diagram displays visually the different transitions.

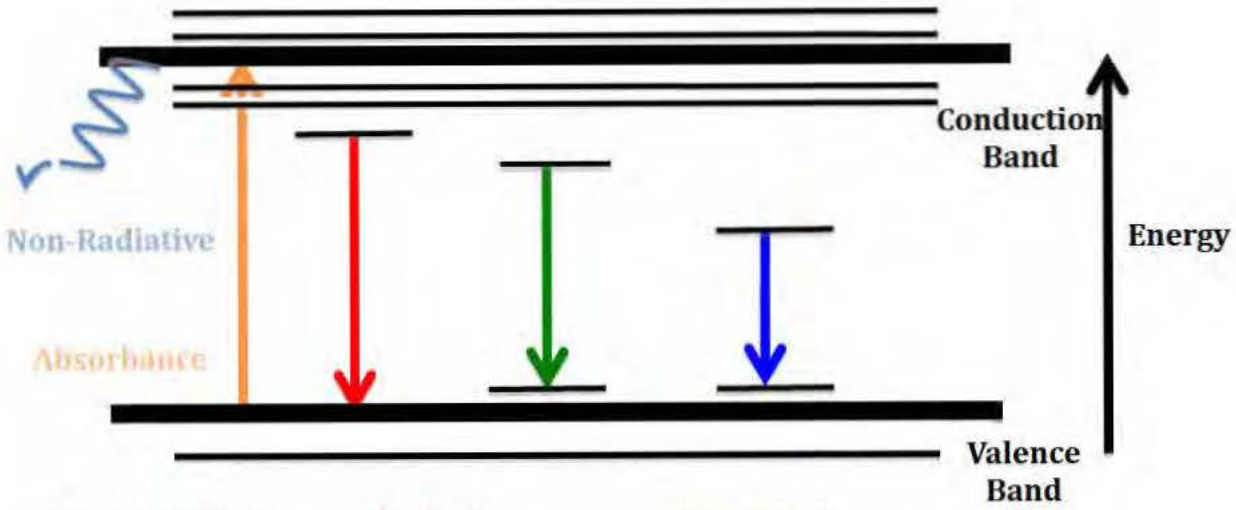

Figure 2. Energy Diagram

Experiment

The main experiment in this study is low temperature photoluminescence excitation. This experiment involves the use of a mechanical vacuum pump and a close cycle He-cryostat. The helium cryostat ranges from temperatures as low as 6K to 300K. Before performing any measurements the quantum dots were mixed with toluene solution. Once the quantum dot dissolved in the solution they were placed on glass slides. The glass slides were coated multiple times so they would display a stronger intensity. After the quantum dots dried on the glass vial, it was then placed into the vacuum chamber. The vacuum chamber decreased the atmospheric pressure and removed all other unwanted gasses while a mechanical pump takes the pressure down to 0.03 Torr in the chamber. After the atmosphere is ~0.03 Torr or less the He-cryostat cycles liquid helium around the chamber is turned on and reduces the temperature to ~6K. A temperature controller system is used to regulate the temperature from 6K to 300K in different intervals. A gold plated clamp that is attached to a brass rod held the glass slides. The gold plate has copper wire attached to it connecting it to the helium unit so it can quickly change the temperature of the glass. Surrounding the brass rod is a steel tube that has 1 window on each of the 4 sides. These windows allows for a variety of spectroscopic studies such as photoluminescence and absorption to be measured. In photoluminescence excitation the samples is placed on a round glass with a 25mm diameter inside the vacuum chamber and the temperature is decreased down to about 6K. The material is then excited by a HeCd UV laser at 325nm. After excitation, the fluorescence is focused by two collimating lenses into a UV fiber optic cable. The fiber optic sends the signals to a spectrometer, which sends the data to a computer and gives a spectral reading based on wavelength and

intensity. Low temperature is a key part of the experiments because at temperatures close to absolute zero, thermal excitations in the quantum dots become minimal. This allows for very precise measurements of emission spectra from laser excitation.

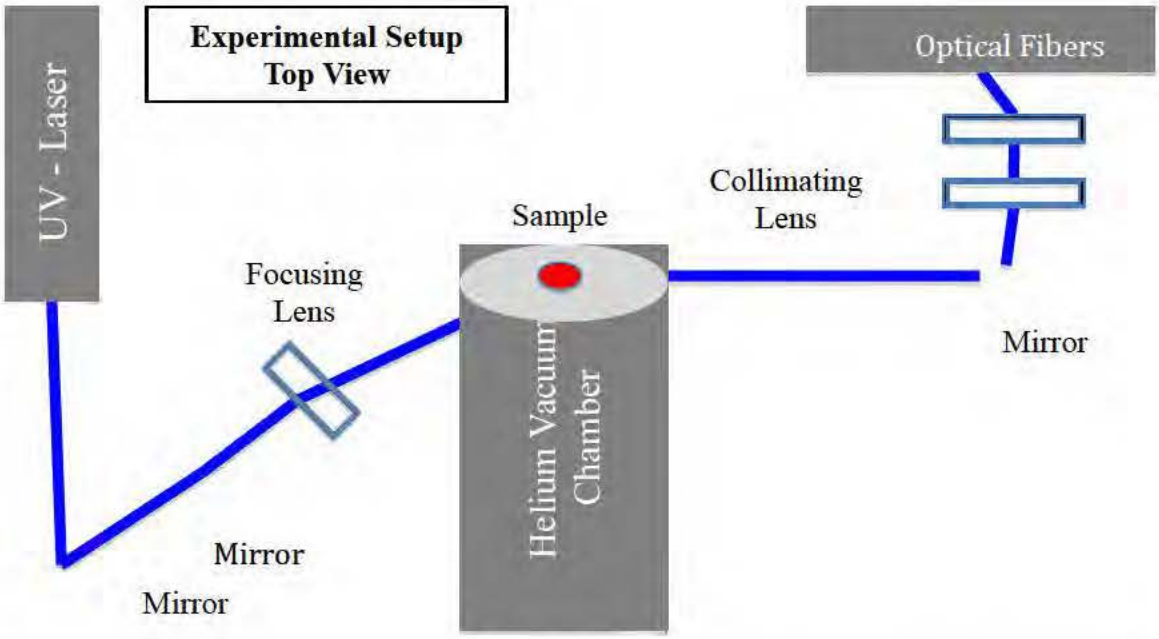

Figure 3. Experimental Setup

Results / Discussion

For the photoluminescence spectra in figure 3(a) the peak emission is at 550nm while 3(b) the peak emission is at 615nm. Figure 3(a) shows the PL spectra that all three transition states contribute to that was discussed in the energy diagram previously. The three major transitions contribute to the spectra at different wavelengths. At higher energies the surface defect related transition is observed. While the intermediate energies correlate to shallow defected related transitions. The final transition observed is deep defect related. A quenching in the spectrum related to the deep defect related transition is observed. This implies that the deep defect related transition state is temperature dependent as to when looking at the shorter wavelengths no surface defect transition is noticed. For the deep defect related transition is possibly due to an Indium atom occupying a copper vacancy. Figure 3(b) displays the photoluminescence spectra of CIS/ZnS 615nm. In this spectra all three energy transitions are present. At shorter wavelengths a narrow spectrum is observed due to the surface related defects. At the surface of the capped quantum dot a sulfur vacancy can attribute to the narrow spectrum. The spectrum quenches around 40K to higher temperatures. This is probably due to Donor-acceptor pair recombination of a sulfur vacancy at the donor level to a copper rich acceptor level.

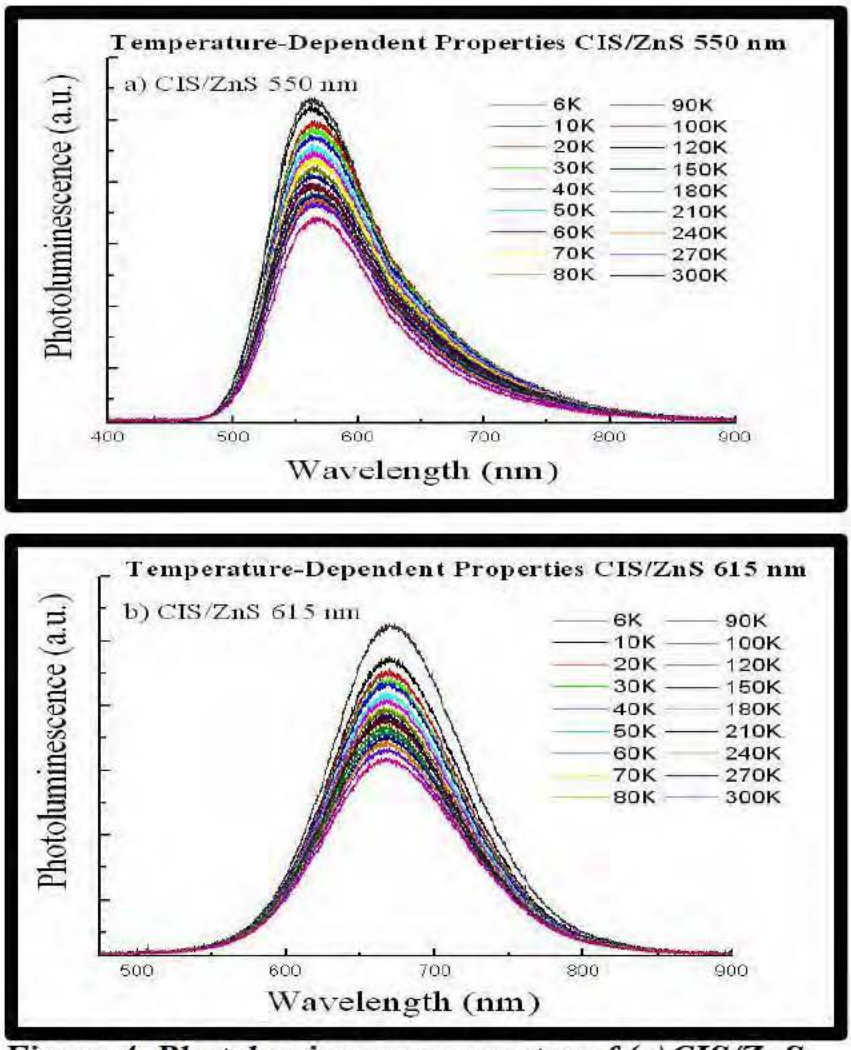

Figure 4. Photoluminescence spectra of (a)CIS/ZnS 550nm (b)CIS/ZnS 615nm at various temperatures, 325nm excitation [China]

Figure 4(a) displays the low temperature photoluminescence spectra of core shell CIS and 4(b) displays the low temperature photoluminescence spectra of core shell CIS capped with ZnS. The role of trap states is evident when looking at the temperature dependent PL spectra. The PL spectra of CIS sample quenched when the temperature was increased above 60 K for the shallow defect related transition. However when capped with ZnS the spectra remained constant with all measured temperatures but the intensity of the PL

increased a little compared to core shell CIS. The quenching of the emission occurs at high temperature by ionization or thermal emptying of the trapping centers if trapped electrons or holes play a role in the non-radiative recombination. Thus the thermal activation energy of quenching process can be related to the ionization energy of the trapping centers. From various reference papers figure 4(c) is the expected photoluminescence spectra of CIS core shell. The coulomb interaction is stronger at the center of the quantum dot therefore the defects that occur inside should remain thermally stable. Quenching occurs at high temperatures due to the optical properties of the sample. At low temperatures the intensity of light is present but as the temperature of the sample is increased the observation of photons decrease because due to the presence of non radiative decay.

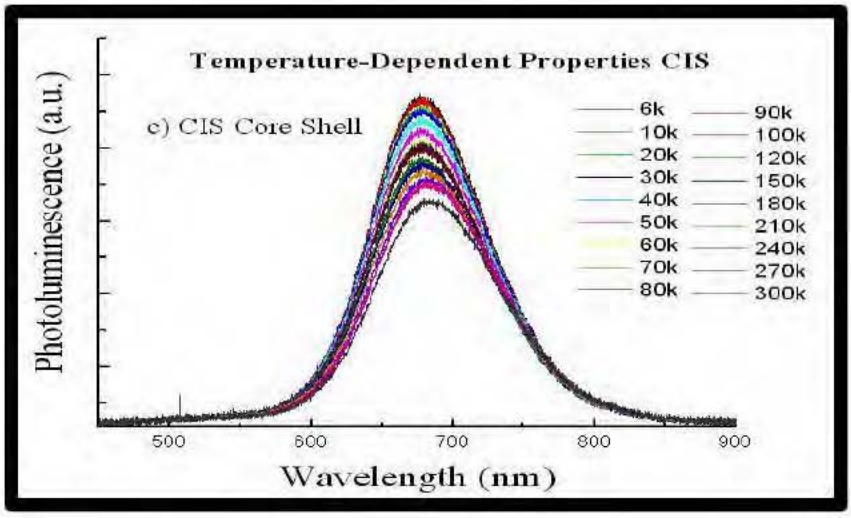

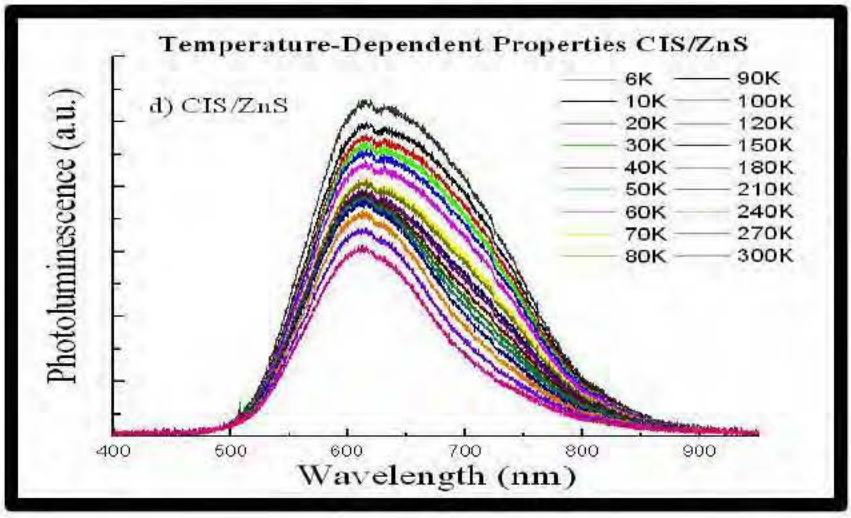

Figure 5. Photoluminescence spectra of (c) CIS core shell (d) CIS/ZnS at various temperatures, 325nm excitation [Korea]

Conclusion

Low-temperature photoluminescence studies of CIS quantum dots in a toluene solution were carried out in temperatures ranging from 6K- 300K. The low range of temperatures allows for the increase in the emission intensity of fluorescence and overall energy change to be observed. As the emission intensity increased observations were made about the transitions states that were present in the quantum dot. The difference in the spectra is most likely due to the surface imperfections, which relates to the different energy states and transition. The interface-defect and surface defect transitions were thermally active at low temperatures. CIS/ZnS the Intrinsic-defect states were relatively stable because the strong Coulomb interaction between charge carriers.

References

[1] Jaetae Seo, Sangram Raut, Mahmoud Abdel-Fattah, Quinton Rice, Bagher Tabibi, Ryan Rich, Rafal Fudala, Ignacy Gryczynski, Zygmunt Gryczynski, Wan-Joong Kim, Sungsoo Jung, and Ryo Hyun, Applied Physics Letters JR13-5367 (2013)

[2] Woo-Seuk Song and Heesun Yang, Applied Physics Letters 100, 183104 (2012).

[3] Yu Zhang, Chuang Xie, Huaipeng Su, Jie Liu, Shawn Pickering, Yongqiang Wang, William W. Yu, Jingkang Wang, Yiding Wang, Jong-in Hahm, Nicholas Dellas, Suzanne E. Mohney, and Jian Xu, Nano Lett. 11, 329 (2011).

[4] Dawei Deng, Yuqi Chen, Jie Cao, Junmei Tian, Zhiyu Qian, Samuel Achilefu, and Yueqing Gu,

[5] Eisberg, R., & Resnick, R. (1985). Quantum physics of atoms, molecules, solids, nuclei, and particles. (2nd ed.). New York: John Wiley & Sons.

[6] Griffiths, D. (2004). Introduction to quantum mechanics. (2nd ed.). New York: Pearson Prentice Hall.

[7] H.Y. Ueng, H. L. Hwang J. appl. Phys. Chem. Solids Vol. 50 No. 12 pp. 1297-1305 (1989)

[8] Chemistry of Materials 24, 3029 (2012).

[9] Quinton Rice Capstone Thesis (2013)

Acknowledgments

The work at Hampton University was supported by the National Science Foundation (NSF HRD-1137747) and Army Research Office (ARO W911NF-11-1-0177). Also Korea Research Institute of Standards and Science for the quantum dot synthesis.

QUINN A. HAILES

3315 West 75th Street
Los Angeles, CA 90043
Email: quinn.hailes@my.hamptonu.edu
Telephone: (310) 654-9160

OBJECTIVE

To perform research and data analysis; areas of particular interest include Optical, Nuclear/Particle, and Medical Physics.

EDUCATION

Bachelor of Science, Physics, Hampton University, Hampton, Virginia
Degree expected May 2014

WORK EXPERIENCE

January 2013 To Present — RESEARCH STUDENT, Physics Department
Hampton University, Hampton, VA
- Conducted research on various Quantum Dots properties
- Constructed Optical Laboratory experiment
- Installed high powered lasers

May 2012 To August 2012 — RESEARCH STUDENT, Physics Department
College of William and Mary, Williamsburg, VA
- Computational work involving the weak charge of a proton, including data analysis of QWEAK conducted at Jefferson Laboratory
- Evaluated raw data with ROOT
- Constructed various objects in machine shop
- Completed advanced radiation training and laboratory safety

May 2011 To August 2011 — RESEARCH STUDENT, Physics Department
University of Notre Dame, South Bend, Indiana
- Computational work involving the half-life of Fe^{60}
- Data acquisition using a Germanium Gamma Ray detector
- Composed spectra to analyze the accelerator and data detectors
- Completed basic radiation training

May 2010 — TEACHER ASSISTANT/MENTOR, Mathematics Department
California State University, Los Angeles
- Led group discussions
- Prepared the class curriculum
- Graded exams for Geometry and Algebra I
- Instructed students in problem solving techniques
- Informed students about the importance of college and STEM fields

June 2009 To August 2009 — RESEARCH STUDENT, Science, Math, Engineering Departments
Hampton University, Hampton, VA
Science Mathematics Engineering Enrichment Program (SMEEP),

- Learned how to problem solve
- Enhanced math, critical thinking, and scientific reasoning skills due to complex class schedule

COMPUTER SKILLS

Linux Operating System
Windows XP Operating Systems
Macintosh Operating Systems
Programs - C++, LATEX, Word, and Excel

AFFILIATIONS

Vice President, Society of Physics Students (SPS)**,** Hampton University chapter
Member, American Physical Society (APS)